Human Pathology (2019) **85**, 65–71

ELSEVIER

Human PATHOLOGY

www.elsevier.com/locate/humpath

Original contribution

Microglandular adenosis is an advanced precursor breast lesion with evidence of molecular progression to matrix-producing metaplastic carcinoma☆,☆☆

Christopher J. Schwartz DO, Igor Dolgalev MS, Esther Yoon MD, Iman Osman MD, Adriana Heguy PhD, Eleazar C. Vega-Saenz de Miera PhD, Diana Nimeh MD, George Jour MD, Farbod Darvishian MD*

New York University Medical Center, New York, NY 10016, USA

Received 13 August 2018; revised 17 October 2018; accepted 24 October 2018

Keywords:
Breast cancer;
Microglandular adenosis;
Metaplastic carcinoma;
Whole-exome sequencing;
TP53;
ADAMTS16

Summary Microglandular adenosis (MGA) is a rare breast lesion reported to be associated with invasive carcinoma in up to 20% to 30% of cases and has been proposed as a nonobligate precursor to basal-like breast cancers. We identified a case of matrix-producing metaplastic carcinoma with morphologic and immunohistochemical evidence of progression from MGA to atypical MGA, carcinoma in situ, and invasive carcinoma. We performed whole-exome sequencing of each component (MGA, atypical MGA, carcinoma in situ, and cancer) to characterize the mutational landscape of these foci. There was a significant copy number overlap between all foci, including a segmental amplification of the *CCND1* locus (partial chromosome 11 trisomy) and *MYC* (8q24.12-13). Using a bioinformatics approach, we were able to identify 3 putative mutational clusters and recurrent, stop-gain nonsynonymous mutations in both *ZNF862* and *TP53* that were shared across all foci. Finally, we identified a novel deleterious splice-acceptor site mutation of chr5:5186164 G>T (chromosome 5p15) encoding the gene, *ADAMTS16*, in the invasive component.

1. Introduction

Microglandular adenosis (MGA) is a rare borderline lesion of the breast characterized by a proliferation of small glands within adipose or fibrous tissue, initially described as a benign histologic, clinical, and radiographic mimicker of invasive carcinoma [1-3]. However, there has been growing evidence over the past 4 decades that MGA can be associated with invasive carcinoma and furthermore serve as a nonobligate precursor lesion to the development of carcinoma [4-11].

Intriguingly, MGA-associated invasive carcinoma is typically triple negative and S100 positive, similar to MGA, pointing to a genetic progression [3,4,6,9]. Molecular studies using comparative genomic hybridization (CGH) and microarray-based CGH have demonstrated copy number alterations that are shared between MGA, atypical MGA (AMGA) and

☆ Competing interests: The authors of this publication have no duality of interests to declare.

☆☆ Funding/Support: The Genome Technology Center is partially supported by the Cancer Center Support Grant P30CA016087 from the Laura and Isaac Perlmutter Cancer Center.

* Corresponding author at: NYU Pathology Associates, 550 1st Ave, Suite TH461, New York, NY 10016.
E-mail address: farbod.darvishian@nyumc.org (F. Darvishian).

https://doi.org/10.1016/j.humpath.2018.10.021
0046-8177/

invasive carcinoma [12-14]. More recent evidence has shown a clonal evolution between MGA and invasive carcinoma using targeted-capture massively parallel sequencing [15]. The defining molecular aberration in MGA and MGA-associated carcinomas is the presence of somatic *TP53* mutation, reportedly occurring in up to 75% of MGA-associated carcinomas [12,15,16].

There is also growing histopathologic evidence that MGA is the precursor lesion to matrix-producing metaplastic carcinoma (MPMC), a rare subtype of metaplastic carcinoma [4,9,17-19]. To our knowledge, no linkage study based on whole-exome sequencing has been done to elucidate the lineage relationship between MGA and MPMC.

We recently identified a case of MPMC, which demonstrated morphologic evidence of transition from MGA to AMGA, carcinoma in situ (CIS), and MPMC. All 4 components retained the defining immunohistochemical marker of MGA, that is, S100 staining and triple-negative phenotype. We applied whole-exome sequencing to characterize the mutational landscape of carcinoma progression.

2. Materials and methods

2.1. Case selection, histochemistry, and immunohistochemistry

We selected a case of a metaplastic carcinoma with mesenchymal differentiation in juxtaposition to foci of MGA, AMGA, and CIS from our institution's archive. Hematoxylin and eosin–stained sections of the case were reviewed independently by 2 breast pathologists (F. D. and D. N.). Immunohistochemistry (IHC) was performed on de-paraffinized, rehydrated sections obtained from each representative focus from formalin-fixed, paraffin-embedded blocks using streptavidin-biotin-peroxidase epitope retrieval using Ventana automated system (Ventana, Tucson, AZ). Antibodies tested include the following: estrogen receptor (ER; clone SP1; Ventana), progesterone receptor (clone 1E2; Ventana), human epidermal growth factor receptor 2 (clone 4B5; Ventana), S100 (clone 4C4.9; Ventana), p53 (DO-7; Ventana), cyclin-D1 (SP4-R; Ventana), epithelial membrane antigen (E29; Cell Marque, Rocklin, CA), calponin (EP798Y; Ventana), and p63 (4A4; Ventana). Histochemical stain for reticulin (silver stain) was performed.

2.2. Macrodissection and DNA extraction

The distinct foci of MGA, AMGA, CIS, and MPMC were carefully outlined by marking the respective foci on the glass slides along with a normal lymph node as control and separately macrodissected from representative 8-μm-thick sections from formalin-fixed, paraffin-embedded blocks. Genomic DNA extraction was performed using QIAamp DNA FFPE Tissue Kit (Qiagen, Germantown, MD).

2.3. Whole-exome sequencing and mutational analysis

Genomic DNA was subjected to whole-exome sequencing (xGen Exome Research Panel v1.0; Integrated DNA Technologies, Coralville, IA; catalog no. 1056115) on Illumina, San Diego, CA HiSeq 4000 platform with a mean coverage of 96-134x of targeted exome regions. The results were demultiplexed and converted to FASTQ format using Illumina bcl2fastq software. The reads were adapted and quality trimmed with Trimmomatic and then aligned to the human reference genome (build hg19/GRCh37) using the Burrows-Wheeler Aligner with the BWA-MEM algorithm according to methods previously described [19-21]. Low-confidence

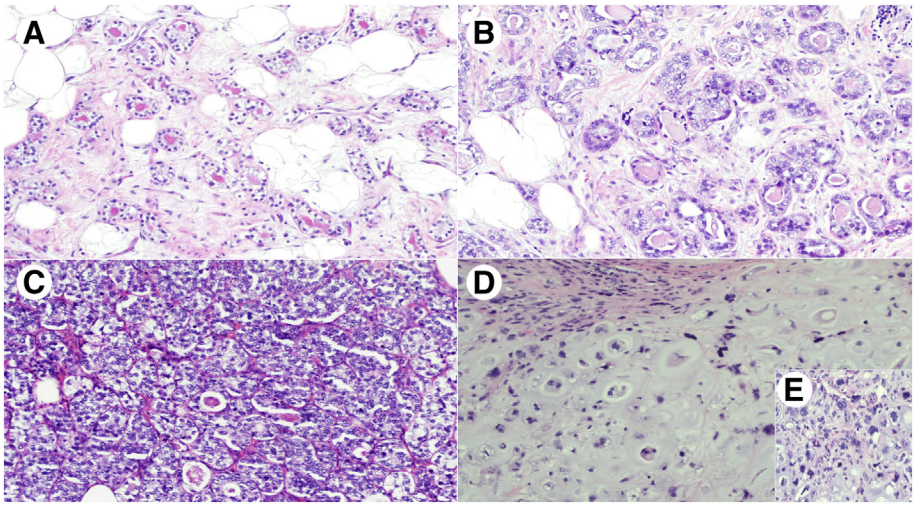

Fig. 1 Representative histologic progression of MGA to MPMC (hematoxylin and eosin). MGA (A, original magnification ×20), AMGA (B, ×20), CIS (C, ×20), and MPMC (D, ×20; E, ×40).

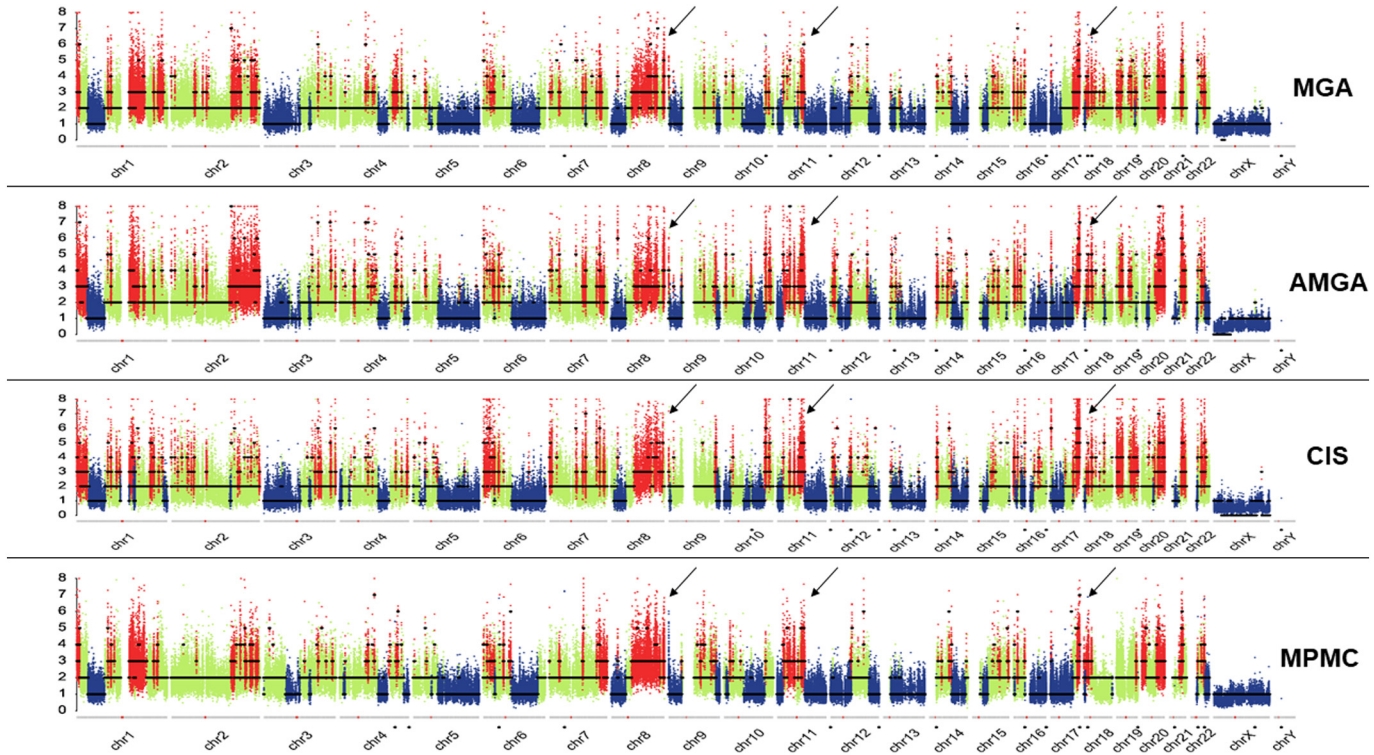

Fig. 2 Copy number profile analysis (non–log scale) demonstrates complex pattern of copy number gains and losses compared with a normal lymph node control. The color coding is based on the predicted copy numbers: red indicates copy number gain, and blue indicates copy number loss. All foci show copy number gains in chromosome 8q, 11q, and 17q (arrowheads). Copy number losses are seen in 1p, 6q, 8q, 9p, 13q, and 16q.

mappings (mapping quality <10) and duplicate reads were removed using Sambamba software v0.6.8 [22]. Further local indel realignment and base-quality score recalibration were performed using the Genome Analysis Toolkit [23]. Single-nucleotide and small indel somatic variants were called with MuTect2. Detection of copy number alterations and allelic imbalances were calculated using Control-FREEC according to methods previously described [24]. PyClone was used to convert the allelic frequency into a cellular prevalence score (CPS) to estimate the relative proportion of lesional cells harboring mutational clusters [25]. ANNOVAR was used to annotate variants with genomic context and functional consequence on genes as well as identify presence in public mutation and pathogenicity databases [26].

2.4. Sanger sequencing

Mutations in *TP53* and *ADAMTS16* were validated using Sanger technique, according to methodology previous described [27].

3. Results

Gross examination of the tumor showed a firm tan-white mass with central hemorrhage, measuring 4.5 × 3 cm. On histologic examination, MGA was composed of round to oval tubules lined by a single layer of cuboidal epithelium distributed haphazardly in fibroadipose tissue. The lumen contained brightly eosinophilic material (Fig. 1A). AMGA was defined as foci of irregular, crowded tubules with less prominent to complete loss of the intraluminal eosinophilic material and evident cytologic atypia manifested by nuclear enlargement, increased nuclear to cytoplasmic ratio, hyperchromasia, pleomorphism, and prominent nucleoli (Fig. 1B) [6]. MGA-CIS demonstrated sheet-like or alveolar growth patterns of cells with cytologic atypia, mitotic activity, and punctate single-cell necrosis (Fig. 1C). The invasive carcinoma was poorly differentiated showing malignant cells with marked cytologic atypia and bizarre, multilobated and "popcorn" nuclei embedded in an extensive extracellular chondroid matrix. There was brisk mitotic activity with numerous atypical mitotic figures (Fig. 1D and E). A clear transition was identified between MGA-AMGA and the accompanying MPMC. MGA and AMGA shared a less defined transition but appeared as distinct regions (Supplementary Fig. 1A and B). The MGA component measured approximately 1.0 cm.

MGA, AMGA, CIS, and associated MPMC displayed S100 protein expression and were negative for ER, progesterone receptor, HER2, and p53 by IHC (data not shown). MGA, AMGA, and CIS showed complete absence of immunoreactivity for calponin and p63 (Supplementary Fig. 2A and B). Epithelial membrane antigen showed variable immunoreactivity in MGA and AMGA in agreement with the literature (Supplementary Fig. 2C) [6]. Reticulin silver stain highlighted the basement membrane around the MGA and AMGA glands (Supplementary Fig. 2D).

The mean DNA coverage was 96x for the normal control (lymph node) and 102-134x for the lesions MGA through MPMC. There was a significant overlap in copy number profiles among all 4 tested entities when compared with lymph node control. All foci shared discrete high amplification in the *CCND1* locus (copy number >4) with associated partial chromosome 11 trisomy. Similarly, there was partial trisomy of chromosome 8q with focal high amplification of 8q24.12-13 encompassing the *MYC* locus. Other segmental events included partial trisomy of 17q25.3 and partial monosomy of chromosomes 1p, 5q, 6q, 8q, 9p, 13q, 16q, and 17p (Fig. 2). These findings highlight the complex genomic aberrations in MGA and further corroborate its relatedness to the corresponding carcinoma. To further validate our findings, we performed

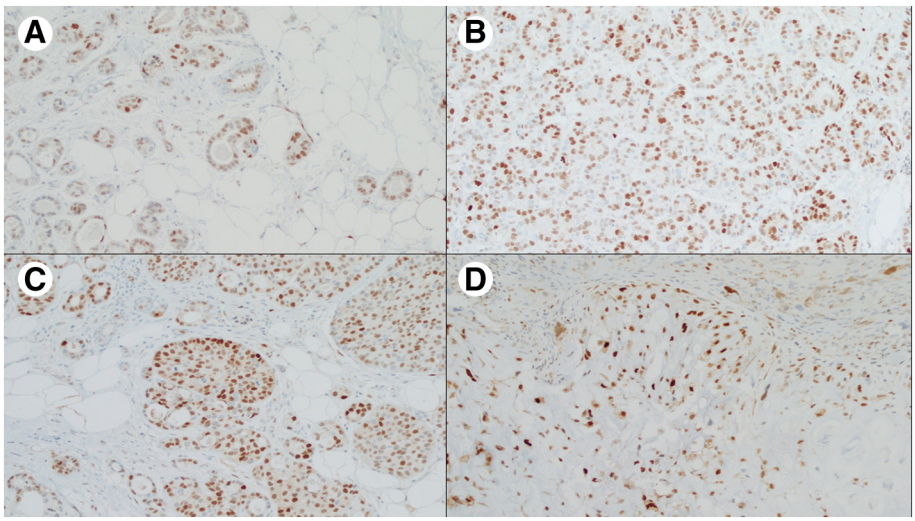

Fig. 3 Representative photomicrographs of MGA (A), AMGA (B), CIS (C), and MPMC (D). Cyclin D1 IHC, original magnification ×20.

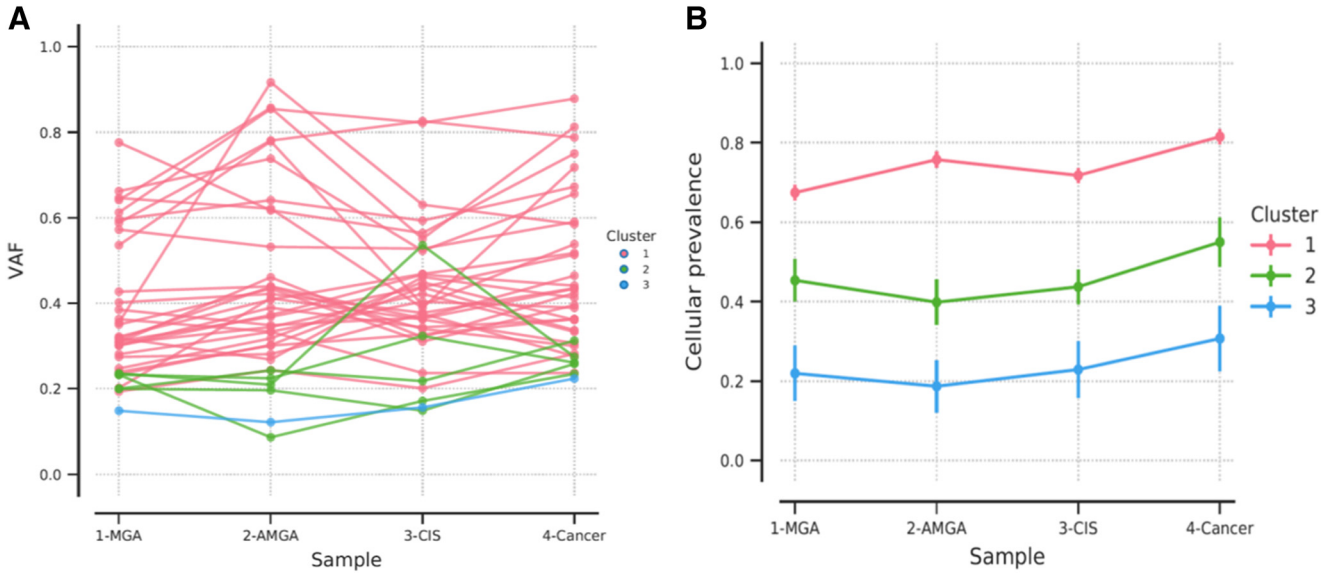

Fig. 4 Prevalence of clonal populations across foci using PyClone. A, Three distinct mutational clusters (1-3) are shared at similar variant allele frequencies across all tested samples. B, The calculated CPS, a refined parameter derived from the VAF used to detect the clusters. The higher the score, the more prevalent is the cluster (set of genes/variants) within the tested tissue. Cluster 1 (red line) is the most prevalent among all 3 detected clusters and is maintained through the evolutionary process from MGA to MPMC. Clusters 2 and 3 represent subclones.

cyclin D1 IHC on the 4 foci of MGA, AMGA, CIS, and MPMC to find a correlate for partial trisomy of chromosome 11. The 4 foci demonstrated diffuse (>50%) and strong nuclear reactivity for cyclin D1 (Fig. 3), whereas the adjacent benign breast tissue showed weak nuclear cyclin D1 labeling (<5%). To investigate clonal evolution between MGA and carcinoma, we used a bioinformatics analysis pipeline (PyClone) that selects genes with similar variant allele frequency (VAF) and builds clusters accordingly. This VAF is converted into a CPS, which represents the strength of a particular cluster. Each cluster can be regarded as a clone [25]. Using this approach, 3 distinct gene clusters were identified as shared among all foci (Fig. 4A). Cluster A featured 29 unique genes and defined a predominant clone that showed the highest prevalence score; clusters B and C had 4 and 1 genes, respectively, and showed a lower prevalence score, indicating their subclonal nature. The list of individual genes contained within each cluster is represented in Supplementary Table.

Within the predominant cluster 1, MPMC showed higher variant allele frequencies and a higher CPS (VAF ranging between 25% and 85%; mean CPS, 0.85; Fig. 3B) compared with MGA (VAF ranging between 25% and 65%; mean CPS, 0.69) for all shared variants. These findings demonstrate that MPMC represents the end result of a clonal evolution and expansion of preexisting MGA.

MGA, AMGA, CIS, and MPMC harbored an expansive repertoire of nonsynonymous somatic mutations, including recurrent *TP53* and *ZNF862* stop-gain mutations observed in all foci (Supplementary Table). Somatic mutation in *TP53* R213X was subsequently verified using Sanger sequencing (Supplementary Fig. 3A). Interestingly, a nonsynonymous point mutation in *ADAMTS16* at chr5:5186164 G>T within the TAG codon was only observed in the carcinoma. This event involves the acceptor splice site at the boundaries of intron 4 and exon 5 and is potentially deleterious to ADAMTS16 protein function. This mutation was subsequently verified using Sanger sequencing (Supplementary Fig. 3B).

4. Discussion

The data herein is the first example of using whole-exome sequencing to analyze MGA, its related lesions, and associated metaplastic carcinoma to provide further validation of its role as a nonobligate precursor to development of triple-negative MPMC. We expand on the complex genetic background of MGA and further support previous studies using CGH and targeted-capture massively parallel sequencing that demonstrated copy number gains in 8q and corresponding 5q/17p losses [12,13,15]. Our findings show that MGA is a genetically advanced lesion with copy number gains in 11q and 17q and partial monosomy in 1p, 6q, 8q, 9p, 13q, and 16q. These copy number alterations were conserved and present in AMGA, CIS, and invasive carcinoma. In keeping with segmental amplification of *CCND1* gene, we identified cyclin D1 protein overexpression in >50% of the nuclei of the lesional cells from MGA to MPMC compared with <5% of the adjacent normal breast lobules. This finding has been observed in ER+ luminal-type breast cancers but rarely in triple-negative breast cancer [28]. Cyclin D1–overexpressing tumors are of prognostic importance as well, as diffuse and strong staining of cyclin D1 may represent a more aggressive phenotype [29].

VAF analysis identified 3 putative mutational clusters that were conserved with increasing frequencies as the lesion

progressed to invasive carcinoma. The largest mutational cluster (cluster 1) showed the highest cellular prevalence compared with the other 2 identified clusters with increasing frequency along the MGA to carcinoma spectrum. This finding suggests that molecular progression from MGA to MPMC involves evolution from a single shared clone (cluster 1), with the other 2 mutational clusters representing divergent subclones. These data are in line with a previous study supporting clonality in MGA-related invasive carcinoma [15].

In agreement with previous studies, we also identified several nonsynonymous point mutations in MGA [12,14-16]. Our study showed a recurrent stop-gain *TP53* R213X mutation that was conserved across all foci. This finding is consistent with previous findings of MGA-associated carcinomas harboring *TP53* mutations albeit at a locus hitherto unreported. In our hands, MGA, AMGA, CIS, and MPMC were completely negative for p53 on IHC, suggesting that premature termination of p53 protein synthesis by stop-gain mutation may render the protein altered or generate a truncated form that is not recognized by the antibody.

We also found a recurrent stop-gain mutation in the *ZNF862* gene. ZNF862 is a zinc-finger protein that may play a role as a transcriptional coactivator of the SWI/SNF-related, matrix-associated, actin-dependent regulator of chromatin (*SMARC2A*). The association with breast carcinoma has not been explored and warrants future investigation.

In addition to *TP53* and *ZNF862*, we found a progressive accumulation of nonsynonymous somatic mutations as MGA progressed to carcinoma. *FAT4* somatic point mutation was found in CIS and MPMC but not in MGA. *FAT4* is a component of the Hippo signaling pathway and has recently been implicated as a tumor suppressor in triple-negative breast cancer [30,31].

An intriguing finding within the mutational profile was a splice-acceptor site mutation of chr5:5186164 G>T (chromosome 5p15) encoding the gene, *ADAMTS16*. This mutation was restricted to the invasive MPMC component. ADAMTS16 protein is a member of the ADAMTS (a disintegrin and metalloproteinase with thrombospondin motifs) protein family and is normally expressed in the developing lung and kidney as well as adult prostate and brain [32]. It is differentially expressed in human synovium and cartilage. In addition, a few members of the ADAMTS family of proteinases include aggrecanases, a group of extracellular proteolytic enzymes whose substrates encompass large proteoglycans in cartilage [33]. In particular, Surridge et al [34] demonstrated that ADAMTS16 overexpression leads to decreased cell proliferation and migration in chondrocytes. In vivo studies have found *ADAMTS16* gene to be downregulated in a chondrosarcoma cell culture line, OUMS-27 [35]. It is tempting to postulate that perhaps a deleterious *ADAMTS16* mutation may lead to dysregulation of the extracellular matrix composition. However, further studies and in vivo modeling are required to support a claim that this gene may play a pathogenic role in the switch from in situ to invasive phenotype.

The limitations of this study are that it involves only a single case. Given the rarity of MGA-associated carcinomas (and even more exceptional MGA-associated MPMC), they are difficult to study. More sequencing data are needed to add to the repertoire of studies that implicate MGA as a nonobligate precursor to invasive carcinoma. However, we believe that this whole-exome sequencing study sheds additional light on the molecular progression of MGA into MPMC and lends further support that MGA can function as a nonobligate precursor to this particularly rare form of breast cancer. Furthermore, we identify *CCND1* amplification with its corresponding abnormal cyclin D1 protein expression in the spectrum of MGA-associated lesions and their corresponding MPMC. Lastly, we describe a novel mutation in *ADAMTS16* gene that warrants further investigation to study its pathogenic role in the development of MPMC.

Supplementary data

Supplementary data to this article can be found online at https://doi.org/10.1016/j.humpath.2018.10.021.

Acknowledgment

We wish to thank members of the NYU Langone Genome Technology Center for expert assistance with whole-exome sequencing.

References

[1] McDivitt RW, Stewart FW, Berg GW. Tumors of the breast. Atlas of Tumor Pathology, Second Series, Fascicle 2. Washington, DC: Armed Forces Institute of Pathology; 1968. p. 91.
[2] Clement PB, Azzopardi JG. Microglandular adenosis of the breast—a lesion simulating tubular carcinoma. Histopathology 1983;7:169-80.
[3] Rosen PP. Microglandular adenosis. A benign lesion simulating invasive mammary carcinoma. Am J Surg Pathol 1983;7:137-44.
[4] Rosenblum MK, Purrazzella R, Rosen PP. Is microglandular adenosis a precancerous disease? A study of carcinoma arising therein. Am J Surg Pathol 1986;10:237-45.
[5] James BA, Cranor ML, Rosen PP. Carcinoma of the breast arising in microglandular adenosis. Am J Clin Pathol 1993;100:507-13.
[6] Koenig C, Dadmanesh F, Bratthauer GL, Tavassoli FA. Carcinoma arising in microglandular adenosis: an immunohistochemical analysis of 20 intraepithelial and invasive neoplasms. Int J Surg Pathol 2000;8:303-15.
[7] Harmon M, Fuller B, Cooper K. Carcinoma arising in microglandular adenosis of the breast. Int J Surg Pathol 2001;9:344.
[8] Salarieh A, Sneige N. Breast carcinoma arising in microglandular adenosis: a review of the literature. Arch Pathol Lab Med 2007;131:1397-9.
[9] Khalifeh IM, Albarracin C, Diaz LK, et al. Clinical, histopathologic, and immunohistochemical features of microglandular adenosis and transition into in situ and invasive carcinoma. Am J Surg Pathol 2008;32:544-52.
[10] Shui R, Yang W. Invasive breast carcinoma arising in microglandular adenosis: a case report and review of the literature. Breast J 2009;15:653-6.

[11] Lee YH, Dai YC, Lin IL, Tu CW. Young-aged woman with invasive ductal carcinoma arising in atypical microglandular adenosis: a case report. Pathol Int 2010;60:685-9.
[12] Shin SJ, Simpson PT, Da Silva L, et al. Molecular evidence for progression of microglandular adenosis (MGA) to invasive carcinoma. Am J Surg Pathol 2009;33:496-504.
[13] Geyer FC, Kushner YB, Lambros MB, et al. Microglandular adenosis or microglandular adenoma? A molecular genetic analysis of a case associated with atypia and invasive carcinoma. Histopathology 2009;55:732-43.
[14] Geyer FC, Lacroix-triki M, Colombo PE, et al. Molecular evidence in support of the neoplastic and precursor nature of microglandular adenosis. Histopathology 2012;60:E115-30.
[15] Guerini-Rocco E, Piscuoglio S, Ng CK, et al. Microglandular adenosis associated with triple-negative breast cancer is a neoplastic lesion of triple-negative phenotype harbouring TP53 somatic mutations. J Pathol 2016;238:677-88.
[16] Geyer FC, Berman SH, Marchiò C, et al. Genetic analysis of microglandular adenosis and acinic cell carcinomas of the breast provides evidence for the existence of a low-grade triple-negative breast neoplasia family. Mod Pathol 2017;30:69-84.
[17] Liu LY, Sheng SH, Zhang ZY, Xu JH. A case of matrix-producing carcinoma of the breast with micoglandular adenosis and review of literature. Int J Clin Exp Pathol 2015;8:8568-72.
[18] Muller KE, Jorns JM. Metaplastic carcinoma with extensive chondromyxoid differentiation arising in association with microglandular adenosis. Int J Surg Pathol 2017;25:513-4.
[19] Kim GE, Kim NI, Lee JS, Park MH. Metaplastic carcinoma with chondroid differentiation arising in microglandular adenosis. J Pathol Transl Med 2017;51:418-21.
[20] Bolger AM, Lohse M, Usadel B. Trimmomatic: a flexible trimmer for Illumina sequence data. Bioinformatics 2014;30:2114-20.
[21] Li H, Durbin R. Fast and accurate short read alignment with Burrows-Wheeler transform. Bioinformatics 2009;25:1754-60.
[22] Tarasov A, Vilella AJ, Cuppen E, Nijman IJ, Prins P. Sambamba: fast processing of NGS alignment formats. Bioinformatics 2015;31:2032-4.
[23] Depristo MA, Banks E, Poplin R, et al. A framework for variation discovery and genotyping using next-generation DNA sequencing data. Nat Genet 2011;43:491-8.
[24] Boeva V, Zinovyev A, Bleakley K, et al. Control-free calling of copy number alterations in deep-sequencing data using GC-content normalization. Bioinformatics 2011;27:268-9.
[25] Roth A, Khattra J, Yap D, et al. PyClone: statistical inference of clonal population structure in cancer. Nat Methods 2014;11:396-8.
[26] Wang K, Li M, Hakonarson H. ANNOVAR: functional annotation of genetic variants from high-throughput sequencing data. Nucleic Acids Res 2010;38:e164.
[27] Sanger F, Nicklen S, Coulson AR. DNA sequencing with chain-terminating inhibitors. Proc Natl Acad Sci U S A 1977;74:5463-7.
[28] Tan DS, Marchió C, Jones RL, et al. Triple negative breast cancer: molecular profiling and prognostic impact in adjuvant anthracycline-treated patients. Breast Cancer Res Treat 2008;111:27-44.
[29] Li Z, Cui J, Yu Q, Wu X, Pan A, Li L. Evaluation of CCND1 amplification and cyclin D1 expression: diffuse and strong staining of CyclinD1 could have same predictive roles as CCND1 amplification in ER positive breast cancers. Am J Transl Res 2016;8:142-53.
[30] Qi C, Zhu YT, Hu L, Zhu YJ. Identification of Fat4 as a candidate tumor suppressor gene in breast cancers. Int J Cancer 2009;124:793-8.
[31] Hou L, Chen M, Zhao X, et al. FAT4 functions as a tumor suppressor in triple-negative breast cancer. Tumour Biol 2016;37:16337.
[32] Cal S, Obaya AJ, Llamazares M, Garabaya C, Quesada V, López-Otín C. Cloning, expression analysis, and structural characterization of seven novel human ADAMTSs, a family of metalloproteinases with disintegrin and thrombospondin-1 domains. Gene 2002;283:49-62.
[33] Nagase H, Kashiwagi M. Aggrecanases and cartilage matrix degradation. Arthritis Res Ther 2003;5:94-103.
[34] Surridge AK, Rodgers UR, Swingler TE, et al. Characterization and regulation of ADAMTS-16. Matrix Biol 2009;28:416-24.
[35] Cakmak O, Comertoglu I, Firat R, et al. The investigation of ADAMTS16 in insulin-induced human chondrosarcoma cells. Cancer Biother Radiopharm 2015;30:255-60.